

# Sol–gel combustion synthesis and characterization of nanostructure copper chromite spinel

Mohammad Hossein Habibi · Fatemeh Fakhri

Received: 21 July 2013 / Accepted: 9 October 2013 / Published online: 30 October 2013  
© Akadémiai Kiadó, Budapest, Hungary 2013

**Abstract** Nanocomposite copper chromite spinel was fabricated by sol–gel process using copper nitrate trihydrate, chromium nitrate nonahydrate, ethylene glycol, diethyl ether, and citric acid. The thermoanalytical measurements (TG–DTG), X-ray powder diffractometry (XRD), field emission scanning electron microscopy (FESEM), and energy dispersive X-ray analysis were used to characterize the structural and the chemical features of the nanocomposites. TG–DTG results showed that the major mass loss for copper(II) nitrate, chromium(III) nitrate as precursors occur at 258 and 140 °C, respectively. The major mass loss for dried gel of copper chromite occurs at 310 °C. XRD data revealed the formation of pure copper chromite after thermal decomposition at 1,000 °C for 2 h. The observation of XRD patterns reveals the presence of single-phase tetragonal spinel  $\text{CuCr}_2\text{O}_4$ . FESEM analysis of calcined composite was found to be in the range of 20–30 nm.

**Keywords**  $\text{CuCr}_2\text{O}_4$  · Copper chromite · Nanocomposite · Spinel

## Introduction

Semiconductor-based nanocomposites are remarkable because of their prospective applications [1–10]. Chromite is a main mineral of chromium, and in Iran it is found in Balochestan and Kerman provinces with about 40 %  $\text{Cr}_2\text{O}_3$

and a chrome-to-iron ratio of 2.6:1 [11–14]. Spinel with the general formula of  $\text{AB}_2\text{O}_4$ , where A and B are cations occupying tetrahedral and octahedral sites, respectively, which A is a divalent and B is a trivalent cations [15–18]. Spinel copper chromite ( $\text{CuCr}_2\text{O}_4$ ) is a narrow band semiconductor used as catalysts for oxidation of carbon monoxide. Different methods are reported for the synthesis of chromite spinels including wet chemical process and micro emulsion processes. Among these methods sol–gel process is a cost-effective which operates at low temperatures and more environmental friendly [19–21]. Previously, we have reported the thermal preparation of semiconductor metal oxides [22–24]. Different methods have also been reported to prepare chromites include [25]. Evaluation of cation influence on the formation of  $\text{M(II)Cr}_2\text{O}_4$  during the thermal decomposition of mixed carboxylate type precursors have been reported [11]. Nanocomposite of chromites has been synthesized by thermal decomposition of precursors [26–29].

The aim of the present study was to develop an environmental friendly sol–gel route to prepare nanosized copper chromite spinel. Moreover, their structural and physical properties were characterized by TG–DTG, X-ray powder diffractometry (XRD), field emission scanning electron microscopy (FESEM), and energy dispersive X-ray analysis (EDAX) techniques.

## Experimental

### Materials and methods

Copper nitrate trihydrate,  $\text{Cu}(\text{NO}_3)_2 \cdot 3\text{H}_2\text{O}$  (2 mmol) and chromium nitrate nonahydrate,  $\text{Cr}(\text{NO}_3)_3 \cdot 9\text{H}_2\text{O}$  (4 mmol) were dissolved in 20 mL distilled water. To the above

M. H. Habibi (✉) · F. Fakhri  
Nanotechnology Laboratory, Department of Chemistry,  
University of Isfahan, Esfahān 81746-73441, Islamic Republic  
of Iran  
e-mail: habibi@sci.ui.ac.ir

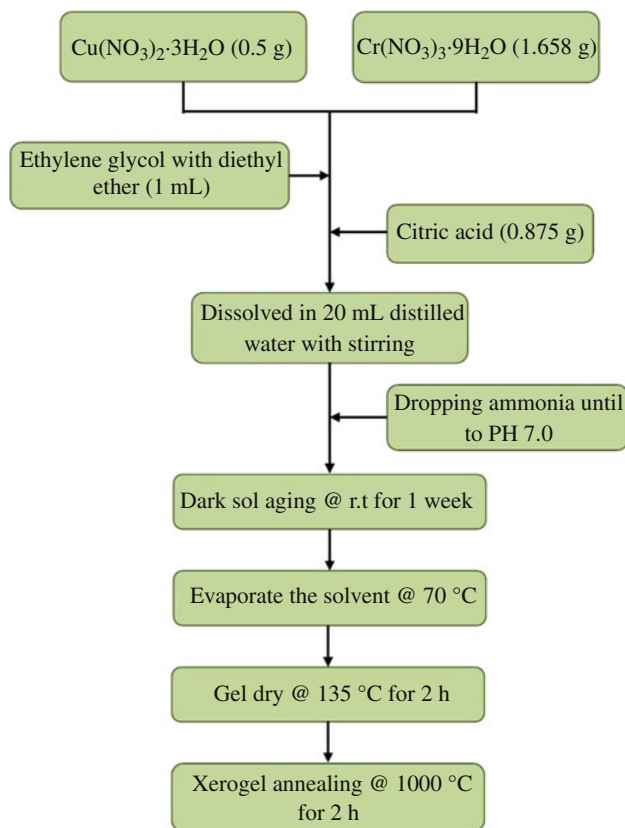


**Fig. 1** Flow chart for preparation of  $\text{CuCr}_2\text{O}_4$  nanocomposites

solution, ethylene glycol (1 mL) and diethyl ether (1 mL) were added and continued stirring. Citric acid (4 mmol) was added to this solution with the molar ratio of citric acid to the Cu of 2:1. After stirring for 30 min, the pH of the solution was adjusted to pH 7.0 by slowly dropping ammonia and continued stirring for 1 h. A homogeneous sol solution was formed which was aged for 1 week at room temperature. The temperature of the obtained stable sol was raised to 70 °C with continued stirring to evaporate the solvent, and the solution turned into high-viscous gel. The gel was then kept at 135 °C for 2 h to allow the Cu–Cr–citric xerogel to form. The xerogel was ignited in air using a few drops of ethanol 96 % as initiating combustion agent. The obtained powder was calcined in air at temperatures ranging from 1,000 °C for 2 h. Figure 1 shows a flow chart of the complete steps sol–gel preparation of nanocomposite copper chromite spinels.

#### Thermal studies

The thermoanalytical measurements (TG–DTG) study for the thermal decomposition of copper nitrate, chromium nitrate, and dried copper chromite sol were carried out with using a Mettler TA4000 system at a heating rate of 10 °C  $\text{min}^{-1}$ . Air at 20 mL  $\text{min}^{-1}$  was used as purge gas.

#### X-ray diffraction

Copper chromite nanoparticles were characterized by XRD analysis using X-ray diffractometer (D8 Advance, BRUKER) in the diffraction angle range  $2\theta = 20^\circ\text{--}60^\circ$ , using Cu  $K\alpha$  radiation. The crystallite size  $D$  of the sample was estimated using the Scherer's equation,  $(0.9\lambda)/(\beta\cos\theta)$ , by measuring the line broadening of main intensity peak, where  $\lambda$  is the wavelength of Cu  $K\alpha$  radiation,  $\beta$  is the full width at half-maximum, and  $\theta$  is the bragg's angle.

#### Field emission scanning electron microscopy

Field emission scanning electron microscopy (FE-SEM, Hitachi, model S-4160) was used to observe the surface morphology of the zinc oxide nanoparticles.

## Results and discussion

#### Thermal investigation

The decomposition mechanism of the  $\text{Cu}(\text{NO}_3)_2\cdot 3\text{H}_2\text{O}$ ,  $\text{Cr}(\text{NO}_3)_3\cdot 9\text{H}_2\text{O}$  precursors, copper chromite xerogel precursor, and the formation of their oxides was studied by thermal analysis. The TG–DTG of copper nitrate, chromium nitrate precursors, and copper chromite xerogel precursor powders are shown in Figs. 2, 3, and 4. The mass loss from room temperature to about 600 °C was 76, 62, and 84 % in the chromium nitrate nonahydrate, copper nitrate trihydrate, and copper chromites, respectively. As shown in Fig. 2 two distinct mass loss centered on 105 and 140 °C are observed for  $\text{Cr}(\text{NO}_3)_3\cdot 9\text{H}_2\text{O}$  as precursors. Figure 3 shows the TG/DTG curves of  $\text{Cu}(\text{NO}_3)_2\cdot 3\text{H}_2\text{O}$  as precursor. A relative mass loss of 10.0 % is observed at 115 °C attributed to the loss of adsorbed water. At 152 °C

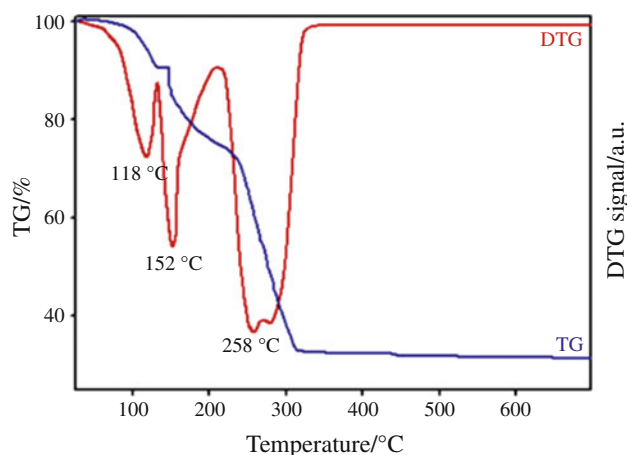


**Fig. 2** TG and DTG curves of  $\text{Cu}(\text{NO}_3)_2\cdot 3\text{H}_2\text{O}$  as precursor

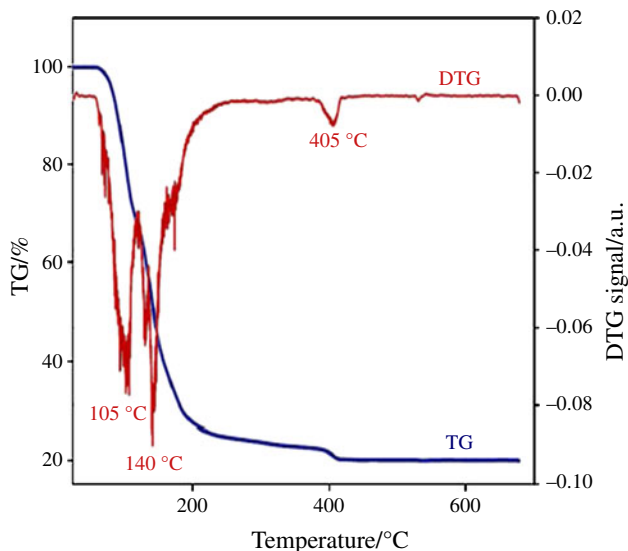


**Fig. 3** TG and DTG curves of  $\text{Cr}(\text{NO}_3)_3 \cdot 9\text{H}_2\text{O}$  as precursor

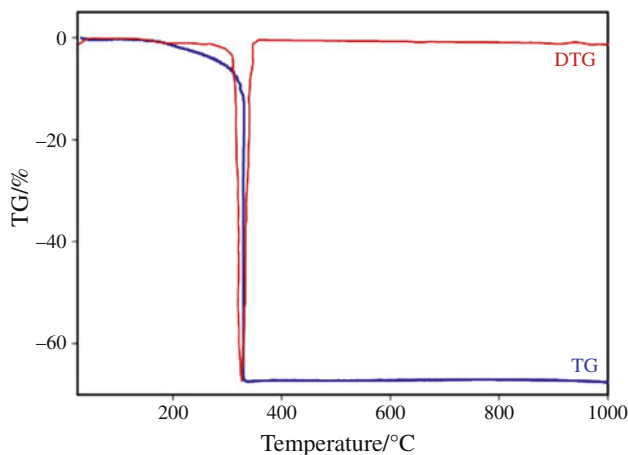


**Fig. 4** TG/DTG curves for dried gel of  $\text{CuCr}_2\text{O}_4$  nanocomposites using  $\text{Cu}(\text{NO}_3)_2 \cdot 3\text{H}_2\text{O}$  and  $\text{Cr}(\text{NO}_3)_3 \cdot 9\text{H}_2\text{O}$  as precursors with mol ratio 1:2 dried at 70 °C

a large mass loss of 15.3 % is observed. A final mass loss is observed at 258 °C of 40.2 %. Figure 4 shows the TG/DTG curves of died gel for  $\text{CuCr}_2\text{O}_4$  precursor. The DTG peak max at 310 °C can be attributed to the decomposition of nitrates and phase transformation to the complete crystallization of copper chromite ( $\text{CuCr}_2\text{O}_4$ ).

X-ray and structural investigation

Figure 5 shows the XRD patterns for copper chromite precursor annealed at 1,000 °C. The xerogel powder is a mixture of amorphous substances and citrate crystals. The XRD patterns of the as burnt powder and powder calcined at 1,000 °C reveal a single phase spinel  $\text{CuCr}_2\text{O}_4$  (PDF No. 34-0424). The XRD pattern shows peaks 18.6 (101), 29.6

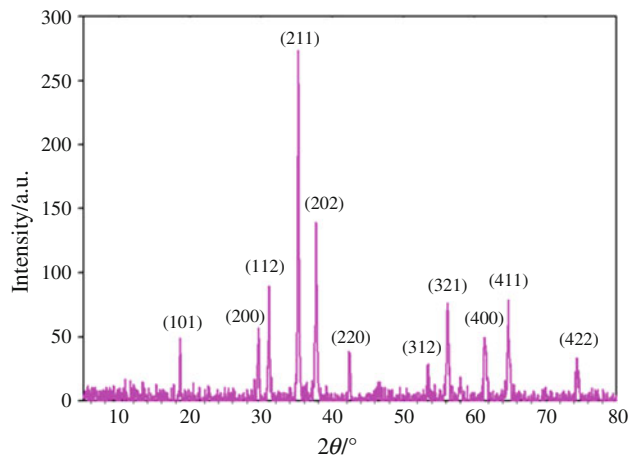


**Fig. 5** XRD pattern of  $\text{CuCr}_2\text{O}_4$  nanocomposite prepared using  $\text{Cu}(\text{NO}_3)_2 \cdot 3\text{H}_2\text{O}$  and  $\text{Cr}(\text{NO}_3)_3 \cdot 9\text{H}_2\text{O}$  as precursors with mol ratio 1:2 annealed at 1,000 °C

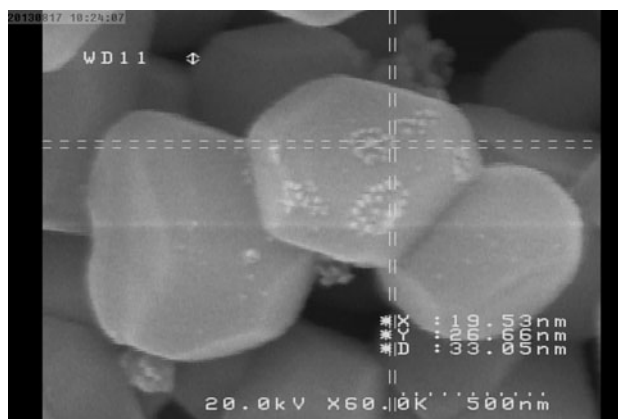


**Fig. 6** FESEM image of  $\text{CuCr}_2\text{O}_4$  nanocomposite prepared using  $\text{Cu}(\text{NO}_3)_2 \cdot 3\text{H}_2\text{O}$  and  $\text{Cr}(\text{NO}_3)_3 \cdot 9\text{H}_2\text{O}$  as precursors with mol ratio 1:2 annealed at 1,000 °C

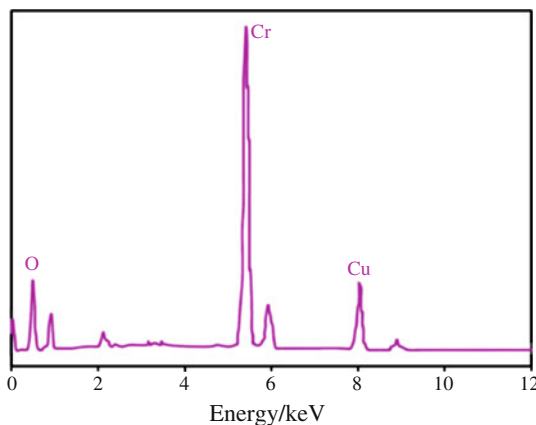


**Fig. 7** EDAX of  $\text{CuCr}_2\text{O}_4$  nanocomposite prepared using  $\text{Cu}(\text{NO}_3)_2 \cdot 3\text{H}_2\text{O}$  and  $\text{Cr}(\text{NO}_3)_3 \cdot 9\text{H}_2\text{O}$  as precursors with mol ratio 1:2 annealed at 1,000 °C

(200), 31.1 (112), 35.2 (211), 42.3 (220), 53.4 (312), 56.2 (321), 61.4 (400), 64.8 (411), and 74.4 (422). The diffraction peaks matched the standard data for  $\text{CuCr}_2\text{O}_4$  (PDF No. 34-0424).

### FESEM analysis

Figure 6 depicts the FESEM micrographs of the powders calcined at 1,000 °C. The micrograph in Fig. 6 shows the formation of powder consisting of octahedral-like structure particles with an average particle size of 20 nm [30]. EDAX spectrum (Fig. 7) corresponding to the single phase spinel  $\text{CuCr}_2\text{O}_4$  calcined at 700 °C indicate the presence of elements Cu, Cr, O in the samples, which further confirms the spinel phase  $\text{CuCr}_2\text{O}_4$ . The EDAX peaks at 1 and 2 eV are assigned to O and Cu.

### Conclusions

The nanocrystalline form of copper chromite was fabricated successfully using a simple, sol–gel method. The influence of calcination temperature on properties was investigated by XRD, FESEM, and TG–DTG. The particle size about 20 nm was formed when the calcination temperature was 1,273 K. EDAX was used to characterize the composition of the samples, and it confirmed the presence of Cu, Cr, and O in the sample. For the first time, we fabricated copper chromite nanoparticles by a simple method. The method can be extended to the fabrication of other spinel chromite nanoparticles of interest in nanotechnology.

**Acknowledgements** The authors wish to thank the University of Isfahan for financially supporting this study.

### References

- Habibi MH, Habibi AH. Effect of the thermal treatment conditions on the formation of zinc ferrite nanocomposite,  $\text{ZnFe}_2\text{O}_4$ , by sol–gel method. *J Therm Anal Calorim.* 2013;113:843–7.
- Habibi MH, Askari E. Synthesis of nanocrystalline zinc manganese oxide by thermal decomposition of new dinuclear manganese(III) precursors. *J Therm Anal Calorim.* 2013;111:1345–9.
- Habibi MH, Askari E. Thermal and structural studies of zinc zirconate nanoscale composite derived from sol–gel process—the effects of heat-treatment on properties. *J Therm Anal Calorim.* 2013;111:227–33.
- Habibi MH, Askari E. The effect of operational parameters on the photocatalytic degradation of CI reactive yellow 86 textile dye using manganese zinc oxide nanocomposite thin films. *J Adv Oxid Technol.* 2011;14:190–5.
- Wu JJ, Tseng CH. Photocatalytic properties of nc-Au/ZnO nanorod composites. *Appl Catal B.* 2006;66:51–7.
- Habibi MH, Mokhtari R. Novel sulfur-doped niobium pentoxide nanoparticles: fabrication, characterization, visible light sensitization and redox charge transfer study. *J Sol Gel Sci Technol.* 2011;59:352–7.
- Lee MS, Hong SS, Mohseni M. Synthesis of photocatalytic nanosized  $\text{TiO}_2$ –Ag particles with sol–gel method using reduction agent. *J Mol Catal A.* 2005;242:135–40.
- Habibi MH, Mikhak M. Synthesis of nanocrystalline zinc titanate ecanodsite by sol–gel: optimization of heat treatment condition for red shift sensitization. *Curr Nanosci.* 2010;7:603–7.
- Iliev V, Tomova D, Todorovska R, Oliver D, Petrov L, Todorovsky D, Unova-Bujnova M. Photocatalytic activity of Ag/ZnO heterostructure nanocatalyst: correlation between structure and property. *Appl Catal A.* 2006;313:115–20.
- Habibi MH, Sheibani R. Preparation and characterization of nanocomposite ZnO–Ag thin film containing nano-sized Ag particles: influence of preheating, annealing temperature and silver content on characteristics. *J Sol Gel Sci Technol.* 2010;54:195–202.
- Barvinschi P, Barbu M, Stoia M, Stefanescu M. Evaluation of cation influence on the formation of  $\text{M(II)Cr}_2\text{O}_4$  during the thermal decomposition of mixed carboxylate type precursors. *J Therm Anal Calorim.* 2013;112:359–66.
- Ștefănescu M, Barbu M, Barvinschi P, Ștefănescu O. The obtaining of  $\text{NiCr}_2\text{O}_4$  nanoparticles by unconventional synthesis methods. *J Therm Anal Calorim.* 2013;111:1121–7.
- Durrani SK, Hussain SZ, Saeed K, Khan Y, Arif M, Ahmed N. Hydrothermal synthesis and characterization of nanosized transition metal chromite spinels. *Turk J Chem.* 2012;36:111–20.
- Rubie DC, Duffy TS, Ohtani E. New developments in high-pressure mineral and applications. San Diego: Elsevier; 2004.
- Gonsalves LR, Mojumdar SC, Verenkar VMS. Synthesis and characterization of ultrafine spinel ferrite obtained by precursor combustion technique. *J Therm Anal Calorim.* 2012;108:859–63.
- Shafa H, Moghadam M, Rahgoshay M, Forouzesh V. Geochemical investigation of nodular chromites in the forumad ophiolite ne of Iran. *Irani J Sci Technol A.* 2009;33:103–8.
- Yaghubpur A, Hassannejad AA. The spatial distribution of some chromite deposits in Iran, using fry analysis. *J Sci Islamic Repub Iran.* 2006;17:147–52.
- Zayat M, Levy D. Blue  $\text{CoAl}_2\text{O}_4$  particles prepared by the sol–gel and citrate–gel methods. *Chem Mater.* 2000;12:2763–9.
- Durrani SK, Qureshi AH, Qayyum S, Arif M. Development of superconducting phases in BSCCO and Ba-BSCCO by sol spray process. *J Therm Anal Calorim.* 2009;95:87–91.
- Durrani SK, Saeed K, Qureshi AH, Ahmad M, Arif M, Hussain N, Mohammad T. Growth of Nd-doped YAG powder by sol spray process. *J Therm Anal Calorim.* 2011;104:645–51.
- Rakesh KS, Yadav A, Narayan A, Singh AK, Verma L, Verma RK. Thermal, structural and magnetic studies on chromite spinel synthesized using citrate precursor method and annealed at 450 and 650 °C. *J Therm Anal Calorim.* 2012;107:197–204.
- Habibi MH, Kiani N. Preparation of single-phase  $\alpha$ -Fe(III) oxide nanoparticles by thermal decomposition. Influence of the precursor on properties. *J Therm Anal Calorim.* 2013;112:573–7.
- Habibi MH, Karimi B. Effect of the annealing temperature on crystalline phase of copper oxide nanoparticle by copper acetate precursor and sol–gel method. *J Therm Anal Calorim.* 2013;. doi:10.1007/s10973-013-3255-4.
- Habibi MH, Askari E. Synthesis, structural characterization, thermal, and electrochemical investigations of a square pyramidal manganese(III) complex with a Schiff base ligand acting as  $\text{N}_2\text{O}_2$  tetradentate in equatorial and as *O* monodentate in axial positions: application as a precursor for preparation of Mn-doped ZnO nanoparticle. *Synth React Inorg Met Org Chem.* 2013;43:406–11.

25. Delmon B. Preparation of heterogeneous catalysts: synthesis of highly dispersed solids and their reactivity. *J Therm Anal Calorim.* 2007;90:49–65.
26. Mirela B, Mircea S, Marcela S, Gabriela V, Paul B. Nanocrystalline InO powders under linear heating conditions. *J Therm Anal Calorim.* 2012;108:1059–66.
27. Stoia M, Barbu M, Stefanescu M, Barvinschi P, Barbu-Tudoran L. Synthesis of nanosized zinc and magnesium chromites starting from PVA–metal nitrate solutions. *J Therm Anal Calorim.* 2012;110:85–92.
28. Da Silva ALA, Castro GGG, Souza MMVM. Synthesis of Sr-doped  $\text{LaCrO}_3$  powders by combustion method: influence of the fuel agent. *J Therm Anal Calorim.* 2012;109:33–8.
29. Barbu M, Stefanescu M, Stoia M, Vlase G, Barvinschi P. New synthesis method for M(II) chromites/silica nanocomposites by thermal decomposition of some precursors formed inside the silica gels. *J Therm Anal Calorim.* 2012;108:1059–66.
30. Geng Q, Zhao X, Gao X, Yang S, Liu G. Low-temperature combustion synthesis of  $\text{CuCr}_2\text{O}_4$  spinel powder for spectrally selective paints. *J Sol Gel Sci Technol.* 2012;61:281–8.